

HIGH GRADIENT INDUCTION ACCELERATOR*[†]

George J. Caporaso[#], S. Sampayan, Y-J. Chen, D. Blackfield, J. Harris, S. Hawkins, C. Holmes, M. Krogh^a, S. Nelson, W. Nunnally^b, A. Paul, B. Poole, M. Rhodes, D. Sanders, K. Selenes^c, J. Sullivan, L. Wang, And J. Watson

Lawrence Livermore National Laboratory, Livermore CA 94551

^aUniversity Of Missouri, 1870 Miner Circle, Rolla, MS 67890

^bUniversity Of Missouri, Columbia, MS 65211

^cTPL Corporation, 3921 Academy Parkway North NE, Albuquerque, NM 87109

Abstract

A new type of compact induction accelerator is under development at the Lawrence Livermore National Laboratory that promises to increase the average accelerating gradient by at least an order of magnitude over that of existing induction machines. The machine is based on the use of high gradient vacuum insulators, advanced dielectric materials and switches and is stimulated by the desire for compact flash x-ray radiography sources. Research describing an extreme variant of this technology aimed at proton therapy for cancer will be described. Progress in applying this technology to several applications will be reviewed.

INTRODUCTION

This paper describes a compact induction accelerator that can have a variety of applications. One concept represents an extreme variant of a high gradient accelerator that has been under development as a compact flash x-ray radiography source [1]. The system is called the Dielectric Wall Accelerator (DWA) and employs a variety of advanced technologies to achieve high gradient. Progress towards the development of this concept is proceeding on several fronts. The key technologies for any DWA are high gradient vacuum insulators, high bulk breakdown strength dielectrics for pulse forming lines, and closing switches compatible with operation at high gradient. In addition, relevant accelerator architectures will be described.

DWA FOR FLASH RADIOGRAPHY

Accelerators for flash x-ray radiography are typically induction linacs that operate at energies on the order of 20 MeV with beam currents of several kiloamperes and pulsewidths of tens of nanoseconds. These electron induction accelerators have average accelerating gradients

on the order of 0.3 – 0.5 MV/Meter. The structure of a typical induction accelerator is shown in Figure 1. Interest in reducing the size and cost of such systems has led to the development of the DWA concept.

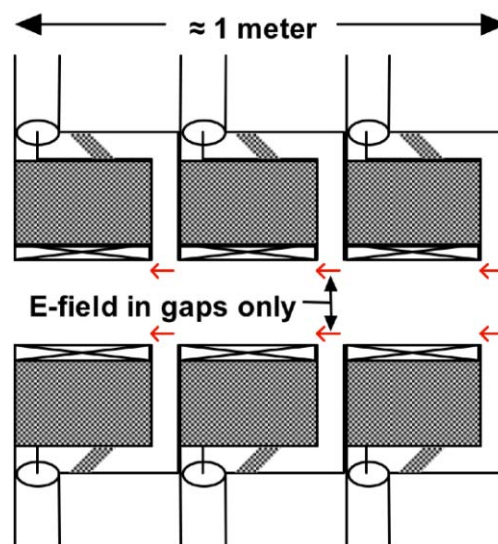


Figure 1: Conventional induction accelerator structure showing three induction modules. The walls are metallic and accelerating fields appear only across the relatively small vacuum gaps. Most of the cell volume is taken up by a magnetic core.

In the typical induction cell the pulsed power is brought in from outside the cell via coaxial transmission lines. A large magnetic core is used to inductively isolate the accelerating gap from the DC short circuit current path that connects each side of the gap. These cores tend to be very large hence limiting the accelerating gradient.

The accelerating gap typically occupies a relatively small fraction of the axial length of the cell yet the field stress in the gap is on the order of 10 – 20 MV/meter for pulses that are tens of nanoseconds long. Since the beam tube is a conductor an accelerating field can only occur in the gap. If we could find an insulator capable of sustaining large electric fields over an extended length then we might be able to make a cell in which the vacuum gap is replaced with this material. If pulse-forming lines could be incorporated inside the cell to feed this insulating

* Multiple patents pending.

[†] This work was performed under the auspices of the U.S. Department of Energy by University of California, Lawrence Livermore National Laboratory under Contract W-7405-Eng-48.

[#] caporasol@llnl.gov

wall a higher gradient accelerating structure might result. Such an arrangement can be found in [1]. It incorporates a “high gradient insulator” (HGI) and a new version of a zero integral pulse-forming line that does not require a magnetic core to produce a net output voltage [2].

HIGH GRADIENT INSULATORS

The leading candidate for the insulating or dielectric wall in the accelerator cell is the High Gradient Insulator (HGI) [3] shown in Figure 2. Vacuum surface flashover is thought to proceed by means of a secondary electron emission avalanche in which field emitted electrons repeatedly bombard the surface of an insulator liberating additional (secondary) electrons and dislodging adsorbed gasses. The electron current ionizes the desorbed gas and eventually forms a dense plasma that shorts out the applied voltage.

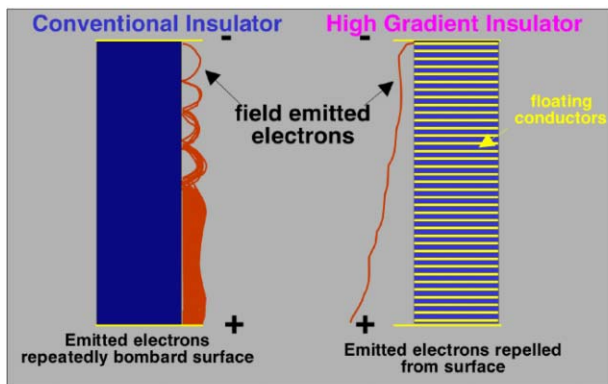


Figure 2: Vacuum surface flashover in conventional straight wall insulators (left) according to generally accepted models along with the situation in high gradient insulators (right). The microstructure of the fields near the surface of the HGI tends to sweep electrons away from the surface [4].

The HGI is composed of standard insulating materials but the configuration is that of thin alternating layers of floating electrodes and insulators usually with periods that are less than one millimeter. The microstructure of the electric fields in the vicinity of the surface tends to sweep secondary electrons away from the insulator resulting in a higher flashover threshold [4]. One of the features of vacuum surface flashover that applies to conventional as well as high gradient insulators is the inverse dependence of the flashover strength on the pulsewidth as is shown in Figure 3. This fact helps to motivate the accelerator architecture for a proton therapy machine discussed in a later section.

The optimum period, composition and aspect ratio (metal to insulator thickness) is still an open question.

Surface breakdown field stress (MV/M) vs. Pulsewidth

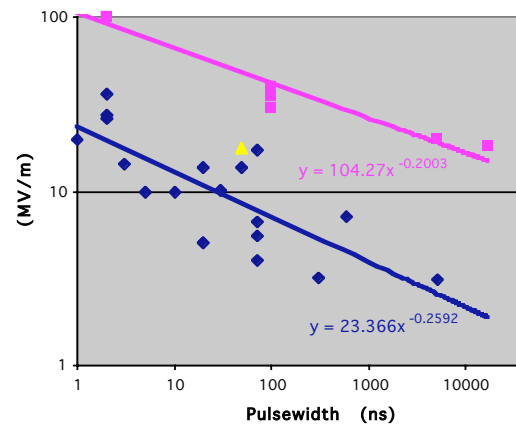


Figure 3: Plot showing surface flashover field stress as a function of pulsewidth for conventional (monolithic) straight wall insulators culled from the literature along with HGI data points showing increased performance.

HGI's have been tested under a variety of extreme conditions. A very early toroidal version (Kapton and stainless steel) 2 cm long by 15 cm inner diameter used as the wall of a simple diode sustained a 420 kV, 20 ns pulse with a 1 kA electron beam passing through its center (a gradient of > 20 MV/m). A more refined Rexolite and stainless steel HGI 1 cm long by 15 cm inner diameter was placed directly across the gap of an ETA-II induction cell and run at 170 kV with a 2 kA, 50 ns electron beam passing through it at 1 Hz for approximately 20,000 shots with no breakdowns. In another test a small disc sample several millimeters (Rexolite and stainless steel) in length withstood 100 MV/m pulses of 3 ns duration [5].

OIL SWITCH DEVELOPMENT

In order to supply the dielectric wall with a tangential electric field used for acceleration some sort of pulse forming line such as the zero integral pulse forming line or other variant must be incorporated into the cell. For any type of pulse forming line a closing switch will be required to launch the pulse. In order to push the performance of pulse forming lines up to high gradient we have been using a simple self-breaking oil switch and a planar Blumlein composed of stainless steel electrodes and either Mylar or polypropylene sheet dielectrics. Using a 50 ns pulse charging system and polypropylene dielectrics reliable operation has been obtained at a dielectric stress of > 100 MV/m for 5 ns pulses.

The entire assembly is immersed in degassed oil. The Blumlein is shown in Figure 4. Because of demanding jitter requirements for the short pulse machine to be described later we are focusing on solid-state switches.

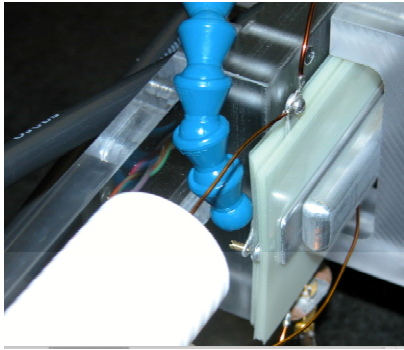


Figure 4: Blumlein with self-breaking oil switch. The line uses sheet insulation of biaxially oriented polypropylene (BOPP) with a total thickness of 2.5 mm per line. The assembly is immersed in degassed oil and can be charged to over 250 kV without breakdown.

SiC PHOTOCONDUCTIVE SWITCH DEVELOPMENT

The ideal closing switch for this application would be capable of high gradient operation with a very long lifetime and a low on resistance. SiC photoconductive switches offer these advantages. The intrinsic bulk breakdown strength of SiC is > 250 MV/m and the switch operates in the linear regime without avalanche or current filamentation. We have built switches from A-plane SiC and tested them up to average field stresses of 27.5 MV/m. Known field enhancements at the edges of the electrodes intensified the field by an order of magnitude and led to failure of the switch above this stress level. This field enhancement will be substantially reduced in the next generation of switches. The switches are fabricated from wafers that are approximately 400 microns in thickness and measure 12 mm by 12 mm. A line focus of laser light is directed into the edge of the switch to activate it [6]. The switches are shown in Figure 5.



Figure 5: SiC photoconductive switches. Each wafer is approximately 400 μ m thick A-plane material with copper electrodes bonded on opposite sides.

CAST DIELECTRIC MATERIAL

Ultimately we would like to use a cast solid dielectric material in the pulse forming lines to simplify the fabrication process and to reduce the cost. For radiographic applications pulses on the order of tens of nanoseconds are required to achieve the desired dose while for the proton therapy application shorter pulses are required. Since the pulsewidth from the pulse forming line is proportional to the square root of the relative dielectric constant it would be desirable to have a material whose properties can be varied for the application. We have been using a material in which high dielectric constant nano-particles are mixed into an epoxy matrix. The effective dielectric constant of the material can be varied by adjusting the concentration of the nano-particles. For low concentrations of the nano-particles, the bulk breakdown strength of the material under DC and pulsed conditions in these small samples is > 400 MV/m. In future tests we will stress larger area samples to assess the bulk breakdown strength. Test samples of the material are shown in Figure 6.



Figure 6: Samples of the cast dielectric material. The brown color material has a low relative dielectric constant (≈ 3) while the light colored material has a high concentration of nanoparticles with a relative dielectric constant of approximately 40.

VIRTUAL TRAVELING WAVE ACCELERATOR

The trends of Figure 3 suggest another possible operating mode of the DWA. The accelerator can be fabricated with a continuous HGI as the beam tube. By controlling the timing of the closing switches in the pulse forming lines a traveling excitation can be applied to the wall. The speed of this excitation can be adjusted to keep pace with a co-moving charged particle so that the particle is continually accelerated through the structure.

Because of the inverse dependence of surface flashover strength on the pulsewidth it is tempting to push operation

to extremely short pulses. However, if this is attempted it will be found that the accelerating gradient on the axis will be substantially less than that along the wall. In order to maintain a high gradient on the axis the beam pulsewidth cannot be too short. In order to evaluate this effect we can use Maxwell's equations to find the on-axis fields given the fields at the wall. Within the beam tube the electric field satisfies the equation

$$\left(\nabla^2 - \frac{\partial^2}{\partial t^2}\right)E_z = 0. \tag{1}$$

Here E_z is the axial component of the electric field. We seek a solution that has an invariant shape as it propagates. We take the field to depend only on the radial position r and on the "retarded time" variable $\tau=t-z/u$ where u is the speed of the wall excitation so that $E_z=E_z(r,\tau)$. Substituting this form into equation (1) and Fourier transforming in τ to the variable ω yields

$$\tilde{E}_z(r,\omega) = \tilde{E}_o(\omega) \frac{I_o\left(\frac{\omega r}{\gamma u}\right)}{I_o\left(\frac{\omega b}{\gamma u}\right)}. \tag{2}$$

Here γ is the usual Lorentz factor, the quantity I_o is the modified Bessel function of order zero and E_o is the Fourier transform of the tangential electric field at the wall. Taking the inverse of equation (2) for a variety of wall excitation waveforms such as a Gaussian, Super Gaussian and hyperbolic secant we obtain a nearly universal curve for the peak on-axis field if we plot against the variable θ defined in Figure 7. The criterion is essentially that the spatial width of the wall excitation must be larger than the beam tube diameter in order that the on-axis gradient be comparable to that along the wall. For beam tube radii on the order of a few cm this criterion implies that the minimum pulsewidth of the accelerator can vary from about 5 ns at the injector down to about 1 ns at the high energy end.

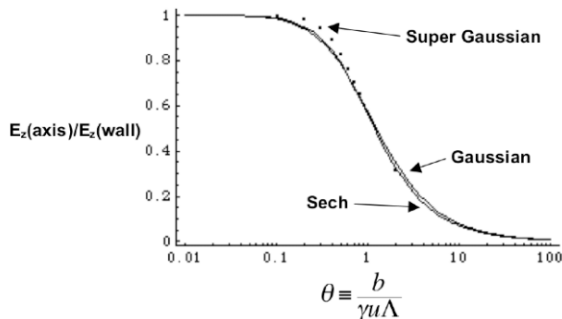


Figure 7: Approximate universal curve giving the ratio of on-axis electric field to that along the beam tube wall as a function of the dimensionless parameter θ for several different temporal wave shapes.

Note that this is an effective, or virtual traveling wave, as the HGI tube does not support such a wave as a natural

transmission mode. The wave is continually forced by wall excitation and so is able to be propagated at any speed. As a consequence, this type of accelerator is capable of accelerating any charged particle.

ACCELERATOR ARCHITECTURES

There are several architectures for the short pulse traveling wave accelerator that appear to be viable. In addition to the zero integral pulse forming line discussed earlier (and variants), stacks of simple Blumleins enclosed in metal container, with or without a magnetic core will produce a large accelerating gradient on-axis. This occurs when the spatial width of the wall excitation is much less than the axial length of the accelerator. A simplified diagram of the accelerator employing Blumlein stacks is shown in Figure 8.

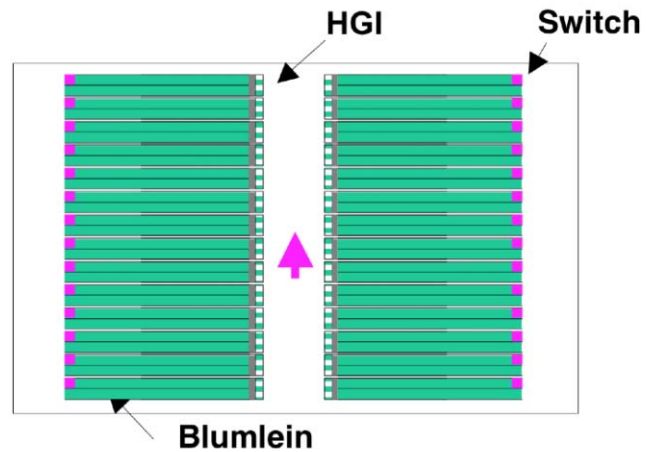


Figure 8: Blumlein stacks surround an HGI. The entire assembly can be enclosed in a metal case without shorting out the voltage if the spatial extent of the excitation on the wall is less than the axial length of the case. Under those conditions the unfired lines act as series loads to the switch end of the Blumlein stack and prevent the collapse of the voltage at that end of the line.

Operation without a magnetic core is possible under the conditions that the axial width of the switched Blumleins is shorter than the axial length of metal enclosure. If this constraint is satisfied the unswitched Blumleins appear as loads in series with the switch ends of the energized Blumleins. The larger the ratio of the axial case length to the length of energized wall the better the result.

The parasitics that limit the performance of this architecture can be eliminated altogether by use of a radial ZIP line (or variants). One drawback of a radial line is that the output pulse is distorted due to the radial variation of impedance. However, the advent of a cast dielectric with adjustable permittivity allows a solution to this problem. By varying the dielectric constant with radius in a prescribed manner the impedance of the line can be made constant. This is just the condition for

dispersionless signal transmission. This is a special case of a more general technique in which the permittivity, permeability and axial width of the lines may all be varied with r in such a manner as to maintain a constant radial impedance as can be deduced from equation (3)

$$Z(r) = \frac{60w(r)}{r} \sqrt{\frac{\mu(r)}{\epsilon(r)}} \quad (3)$$

Any combination of parameter variation that maintains constant impedance will yield distortionless transmission. A special case restricting the variation to the relative dielectric constant only gives the prescription

$$\epsilon(r) = \epsilon_{\min} \left(\frac{b}{r}\right)^2 \quad (4)$$

where b is the outer radius of the line and ϵ_{\min} is minimum value of the permittivity. The variation in dielectric constant can be accomplished using a finite number of discrete steps and yields flat waveforms [7]. These lines are very low impedance and are suitable for very high beam currents.

In order to make a dramatic change in the paradigm for proton therapy we are attempting to make an accelerator so compact that it would fit in a single treatment room in a small clinic. To accomplish this we are aiming at an average accelerating gradient of 100 MV/m. With a gradient this large space charge-induced expansion of a 100 mA proton beam will be insignificant during the 25 ns transit time through the accelerator. A compact spark discharge proton source can be used along with an arrangement of several electrodes to independently control the extracted current and final spot size on each pulse [8]. The focusing takes place in the space between the source and the entrance to the accelerator. In addition, the beam energy can be adjusted on each pulse. A diagram illustrating the concept is shown in Figure 9.

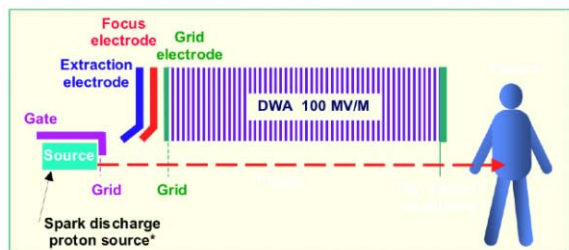


Figure 9: A spark discharge source provides the protons through a small aperture. Extraction and focusing electrodes are used to control intensity and spot size.

The accelerator system can be configured in various ways to treat patients. The accelerator can be mounted on a gantry in an isocentric configuration or it could be mounted vertically or nearly horizontally. One of these possibilities is shown in Figure 10.

The repetition rate for the accelerator can be tens of Hertz and would be limited by thermal effects in the switches [9].

The next steps in the development of this concept over the next year and a half are to bring the performance

levels of the components and the accelerator architectures up to the point that an integrated system can achieve 100 MV/m. Once this has been achieved we want to demonstrate the performance of an integrated system, a *sub-scale prototype* at the 10 MeV level.

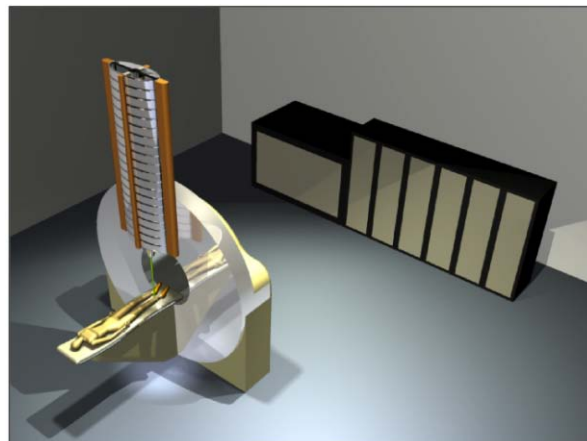


Figure 10: Compact proton therapy concept. The goal is to mount a compact linac on a gantry that can fit into a standard, conventional linac vault.

CONCLUSION

We have described the DWA concept, discussed the insulator, switch and dielectric technologies necessary to reach high gradients and have presented a short pulse, virtual traveling wave architecture that we are exploring for proton therapy applications.

REFERENCES

- [1] G. Caporaso, "New Trends in Induction Accelerator Technology", Proc. Int. Workshop. Recent Progress in Induction Linacs, Tsukuba, Japan, 2003.
- [2] M. Rhodes, "Ferrite-Free Stacked Blumlein Pulse Generator for Compact Induction Linacs", in Proc. IEEE. International Pulsed Power Conf., (2005).
- [3] S. Sampayan, et. al., IEEE Trans. Diel. and Elec. Ins. 7 (3) pg. 334 (2000).
- [4] J. Leopold, et. al., IEEE Trans. Diel. and Elec. Ins. 12, (3) pg. 530 (2005).
- [5] W. Nunnally, et. al., Proc. 14th IEEE Int. Pulsed Power Conf. PPC-2003, pg. 301 (2003).
- [6] J. Sullivan and J. Stanley, "6H-SiC Photoconductive Switches Triggered Below Bandgap Wavelengths", in Proc. 27 Int. Power Modulator Symposium and 2006 High Voltage Workshop, Washington, D.C. 2006.
- [7] S. D. Nelson, et al., "Electromagnetic Simulations of Linear Proton Accelerator Structures using Dielectric Wall Accelerators," these proceedings.
- [8] Y.-J. Chen and A. C. Paul, "Compact Proton Accelerator for Cancer Therapy", these proceedings.
- [9] L. Wang, et al., "Electromagnetic and Thermal Simulations for the Switch Region of a Compact Proton Accelerator," these proceedings.